FicD sensitizes cellular response to glucose fluctuations in mouse embryonic fibroblasts

Burak Gulen[a,b,1], Aubrie Blevins[a,1], Lisa N. Kinch[a,b] (ID), Kelly A. Servage[a,b] (ID), Nathan M. Stewart[a,b], Hillery F. Gray[a,b], Amanda K. Casey[a,b] (ID), and Kim Orth[a,b,c,2] (ID)

Affiliations are included on p. 11.

During homeostasis, the endoplasmic reticulum (ER) maintains productive transmembrane and secretory protein folding that is vital for proper cellular function. The ER-resident HSP70 chaperone, binding immunoglobulin protein (BiP), plays a pivotal role in sensing ER stress to activate the unfolded protein response (UPR). BiP function is regulated by the bifunctional enzyme filamentation induced by cyclic-AMP domain protein (FicD) that mediates AMPylation and deAMPylation of BiP in response to changes in ER stress. AMPylated BiP acts as a molecular rheostat to regulate UPR signaling, yet little is known about the molecular consequences of FicD loss. In this study, we investigate the role of FicD in mouse embryonic fibroblast (MEF) response to pharmacologically and metabolically induced ER stress. We find differential BiP AMPylation signatures when comparing robust chemical ER stress inducers to physiological glucose starvation stress and recovery. Wildtype MEFs respond to pharmacological ER stress by down-regulating BiP AMPylation. Conversely, BiP AMPylation in wildtype MEFs increases upon metabolic stress induced by glucose starvation. Deletion of FicD results in widespread gene expression changes under baseline growth conditions. In addition, FicD null MEFs exhibit dampened UPR signaling, altered cell stress recovery response, and unconstrained protein secretion. Taken together, our findings indicate that FicD is important for tampering UPR signaling, stress recovery, and the maintenance of secretory protein homeostasis.

AMPylation | Fic enzymes posttranslational modifications | unfolded protein response | ER stress | BiP

Cellular stress responses alter the balance of protein synthesis, modification, and degradation in the cell to maintain protein homeostasis and cellular function. The unfolded protein response (UPR) is an adaptive signaling pathway that helps to restore cellular homeostasis to varying levels of endoplasmic reticulum (ER) stress (1), ranging from mild to maladaptive (2). Activation of the UPR is regulated by the essential ER chaperone protein BiP [a.k.a. glucose regulated protein 78 or heat shock protein family A member 5 (Hspa5)] and results in the activation of a complex signaling network promoting both cell survival and apoptosis pathways (3–5). As the main chaperone residing in the ER, BiP plays a critical role in promoting both the correct folding and transport of newly synthesized proteins passing through the ER and the degradation of misfolded proteins by the ER-associated protein degradation (ERAD) pathway (1). The UPR is activated when the ER protein folding capacity is insufficient to cope with the burden of unfolded proteins accumulating in the ER (6). UPR aims to restore homeostasis by attenuating global translation and transcription, and by enhancing the folding capacity of the cell through selective transcription and translation of chaperones like BiP (7, 8).

UPR is activated by the three transmembrane ER stress sensors that serve as distinct yet intertwined signaling branches: 1) PERK [protein kinase RNA (PKR)-like ER kinase], 2) IRE1α (inositol-requiring enzyme 1α), and 3) ATF6 (activating transcription factor 6) (1, 3). When unfolded proteins accumulate in the ER lumen, BiP dissociates from the three signal transducers to implement the UPR (1, 4) (Fig. 1A). PERK phosphorylates eIF2α to repress protein synthesis and induce preferential translation of Atf4, the master transcription factor of the integrated stress response. Ire1α processes unspliced *X-box binding protein 1* (*XBP1*) mRNA, promoting the translation of the XBP1 transcription factor, which up-regulates ER chaperones and ERAD components. Membrane-bound Atf6 translocates from the ER to the Golgi apparatus, where it is processed into a cytoplasmic transcription factor that up-regulates ER chaperones and lipid synthesis. The regulation of transcription during UPR is critical for normal cellular function and health; however, failure to restore homeostasis ultimately leads to a maladaptive/pathologic phase encompassing activation of proapoptotic genes and programmed cell death (Fig. 1A).

Significance

The chaperone BiP plays a key quality control role in the endoplasmic reticulum, the cellular location for the production, folding, and transport of secreted proteins. The enzyme FicD regulates BiP's activity through AMPylation and deAMPylation. Our study unveils the importance of FicD in regulating BiP and the unfolded protein response (UPR) during stress. We identify distinct BiP AMPylation signatures for different stressors, highlighting FicD's nuanced control. Deletion of FicD causes widespread gene expression changes, disrupts UPR signaling, alters stress recovery, and perturbs protein secretion in cells. These observations underscore the pivotal contribution of FicD for preserving secretory protein homeostasis. Our findings deepen the understanding of FicD's role in maintaining cellular resilience and open avenues for therapeutic strategies targeting UPR-associated diseases.

[1]B.G. and A.B. contributed equally to this work.

[2]To whom correspondence may be addressed. Email: kim.orth@utsouthwestern.edu.
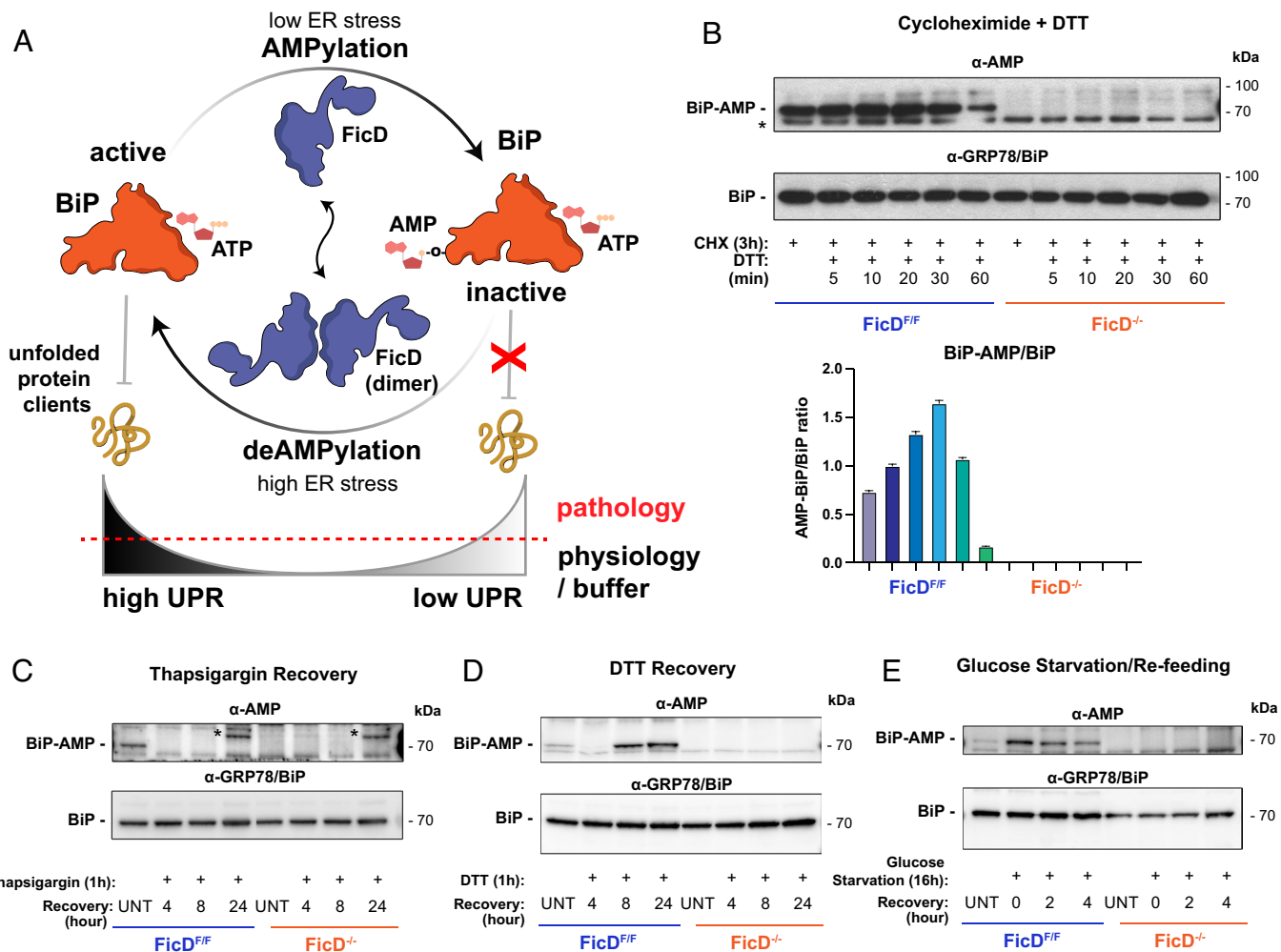
Fig. 1. AMPylation of BiP and response to ER stress in MEFs. (*A*) Regulation of BiP activity by AMPylation. Oligomeric state of FicD mediates the antagonistic activities of FicD (12, 13). (*B*) AMPylation responds to ER stress in *FicD*^F/F MEFs and *FicD*^−/− MEFs. Western blots showing AMPylated and total BiP. After 3 h of cycloheximide (CHX, 100 μg/mL) treatment. Adding DTT (1 mM) in CHX treated MEFs increases the ER stress and thus decreases the AMPylation of BiP over time. *FicD*^−/− cells do not show BiP AMPylation in the absence of FicD. *unidentified band, present in both genotypes. Bar graph representation of the BiP-AMP/BiP ratio. (*C*–*E*) Western blots showing AMPylated and total BiP. *unidentified band, present in both genotypes. MEFs are treated with ER stressing drugs (*C*) TG (1 μM) or (*D*) DTT (1 mM) for 1 h or (*E*) starved for glucose for 16 h following the recovery by either removing the drug or adding glucose. UNT: untreated/unstressed.

Chronic or dysregulated UPR is associated with a variety of diseases (9–11).

AMPylation [i.e., adenosine monophosphate (AMP) transfer to proteins] is a posttranslational modification (PTM) conserved across all kingdoms of life. Catalyzed primarily by the large family of filamentation induced by cyclic-AMP (Fic) enzymes (14–21), AMPylation modulates cellular functions (22), typically resulting in inactivation of target proteins. Metazoans carry a single Fic domain protein-encoding gene (*FicD*). *FicD* encodes a bifunctional enzyme localized in the endoplasmic reticulum (ER) membrane with a luminal catalytic domain (23) that reversibly AMPylates or deAMPylates the ER chaperone BiP (24, 25). In a state of homeostasis, FicD acts as an AMPylator, generating an inactive reserve pool of the BiP chaperone within the ER lumen (26–28). During ER stress, deAMPylation of BiP by FicD reactivates this pool of chaperones to aid in resolving stress induced by unfolded proteins (29).

Alternate proposals exist in the field pertaining to the fitness benefits of FicD-dependent BiP AMPylation. Some studies anticipate that AMPylation of BiP acts as a molecular rheostat for UPR. The rheostat allows different cells to respond to varying ER stress thresholds by maintaining excess BiP in a reversibly inactive state (14, 15, 24, 29). Previous studies using animal models support this hypothesis, as loss of FicD results in aberrant UPR signaling in

tissues and sensitizes tissues to damage in *Drosophila*, *Caenorhabditis elegans*, and mice (30–32). Of note, heterozygous FicD^+/− mice or flies exhibit behaviors similar to wild type as demonstrated by previous work (30, 31). In the absence of FicD, tissues facing repetitive stress display increased damage and delayed recovery after each insult (31). AMPylation and rapid inactivation of BiP have also been suggested to benefit cells by preventing overchaperoning and excessive ERAD pathway activation (33). This hypothesis is supported by AMPylation profiles of BiP in cells that correlate with UPR activation and by in vitro kinetic modeling of protein-folding homeostasis in the ER with and without a reserve source of BiP for fast reactivation (24, 28, 34). Despite these previous studies, key questions remain regarding how specific cellular stresses induce changes in BIP activity.

We sought to better define the fitness role of FicD in mammalian cells experiencing physiological and pharmacological-induced ER stress. We recently produced a floxed, Flag-tagged *FicD* allele in mice to study the effect of FicD in response to ER stress and found that loss of FicD leads to elevated UPR and reduced recovery from ER stress (31). Here, we isolated and immortalized control Flag-tagged FicD mouse embryonic fibroblasts (MEFs) and FicD knockout MEFs (*FicD*^F/F MEFs and *FicD*^−/− MEFs, respectively) (*SI Appendix*, Fig. S1) to characterize the role of FicD in response to ER stress at

a cellular level. Using a variety of methods, we report that the absence of FicD causes fundamental changes in the transcriptome, leading to increased expression and secretion of extracellular matrix (ECM) proteins. The *FicD*^{−/−} MEFs lack a transcriptional response to glucose starvation and display a dampened transcriptional UPR. Taken together, our data support the hypothesis that AMPylation of BiP tempers the activation of the UPR response under physiological ER stress-inducing conditions.

Results

MEFs Undergo Reversible AMPylation of the ER Chaperon BiP.

To study the cellular response to BiP AMPylation, FLAG-tagged *FicD*[F/F] MEFs and *FicD*^{−/−} mutant MEFs were isolated, cultured, and immortalized by transfection with SV40 antigen–containing plasmid. While the limited expression levels of FicD did not allow its endogenous detection through western blots, FicD can be monitored both at the transcript and enzymatic activity levels. Using both RT-qPCR of *FicD* transcript and assessment of BiP-AMPylation levels via Western blot analysis, we observed that immortalized *FicD*[F/F] MEFs grown in standard growth media produce *FicD* mRNA and functional FicD enzyme capable of reversibly AMPylating BiP, whereas the *FicD*^{−/−} MEFs do not express *FicD* or AMPylate BiP (Fig. 1*B* and *SI Appendix*, Fig. S2).

Previously, we have shown that CHX treatment, which inhibits mRNA translation, enhances BiP AMPylation in cell lines (24). To determine how loss of FicD influences this response, we treated our immortalized *FicD*[F/F] and *FicD*^{−/−} MEFs with CHX. Consistent with previous observations, BiP AMPylation increases in *FicD*[F/F] MEFs following CHX exposure as monitored by western blots using monoclonal α-AMP antibody. Unlike control cells, *FicD*^{−/−} MEFs exhibited no detectable BiP AMPylation (Fig. 1*B*) (24). Next, we perturbed the ER's oxidation state in CHX-treated cells by introducing the reducing agent DTT into the culture media. This treatment results in the reversal of BiP AMPylation in *FicD*[F/F] MEFs over time (60 min; Fig. 1*B*), indicating that BiP AMPylation levels change in response to different cellular stresses, even when global protein synthesis levels are inhibited.

Next, we surveyed the AMPylation status of BiP during recovery from ER stress caused by treatment with thapsigargin (TG) or DTT alone. TG inhibits the sarco/ER Ca^{2+} ATPase, thereby perturbing Ca^{2+} signaling in the ER (35). Following exposure to either TG or DTT, MEFs were allowed to recover from ER stress in fresh media. Unstressed cells exhibit a baseline AMPylation level of BiP, which disappears in response to both pharmacological ER stress treatments (Fig. 1 *C* and *D*). Irreversible TG-mediated stress results in a loss of BiP AMPylation that persisted even after 24 h of recovery. By contrast, MEFs recovering from reversible DTT-mediated ER stress display a reemergence of BiP AMPylation at around 8 h (Fig. 1*D*). The protein levels of BiP do not change significantly under these conditions (Fig. 1 *C* and *D*).

In addition to these pharmacological stressors, we sought to study a physiological stress condition in MEFs by depriving cells of glucose in the growth media. Glucose starvation is an established physiological stress that leads to induction of the UPR (2, 36, 37). Interestingly, glucose starvation in *FicD*[F/F] MEFs resulted in a behavior like that observed upon CHX treatment, boosting BiP AMPylation. After adding back glucose to the media, the AMPylation levels decreased toward the baseline exhibited by unstressed cells (Fig. 1*E*).

FicD^{−/−} MEFs Exhibit Altered UPR Gene Expression Patterns during Stress and Recovery.

To complement our analysis of BiP AMPylation during an ER stress, we used RT-qPCR to measure how mRNA levels of UPR genes change during various stress-inducing conditions in

the *FicD*[F/F] and *FicD*^{−/−} MEFs. We predicted that UPR signaling and recovery in *FicD*[F/F] and *FicD*^{−/−} MEFs may be differentially altered under these various conditions in the presence and absence of BiP AMPylation (Fig. 1 *C–E*).

Treatment with TG for over 1-h increased the levels of *Atf3* and s*Xbp1* transcripts in *FicD*[F/F] MEFs, and their relative expression was significantly higher in *FicD*^{−/−} MEFs across all time points. In contrast, relative expression levels of *Chop/Ddit3* and *Atf4* increased to the same extent in both genotypes (Fig. 2*A* and *SI Appendix*, Fig. S2*A*). Additionally, expression patterns of the *BiP/Hspa5* transcript differed significantly between *FicD*[F/F] and *FicD*^{−/−} MEFs during TG treatment. Over the 1-h treatment with TG, expression levels of the *BiP/Hspa5* transcript steadily increased in *FicD*[F/F] MEFs. However, in *FicD*^{−/−} MEFs expression levels of the *Bip/HspA5* transcript were significantly diminished within the first 15 min of treatment and remained significantly diminished during the 1-h TG treatment (*SI Appendix*, Fig. S2*A*). These data support the proposal that induction of UPR by acute TG treatment was differentially regulated in *FicD*[F/F] and *FicD*^{−/−} MEFs.

We next analyzed how *FicD*[F/F] and *FicD*^{−/−} MEFs recovered from stress by treating cells with DTT followed by washing and observing gene expression after 4, 8, and 24 h of recovery. The mRNA for *Atf3*, *Chop/Ddit3*, and s*Xbp1* decreased over time to baseline levels (after 24 h of recovery). In the early (4-h) recovery timepoint, the levels of *Atf3*, *Chop/Ddit3*, and *BiP/HspA5* transcripts were significantly higher in *FicD*^{−/−} cells, suggesting a delayed recovery from UPR in *FicD*^{−/−} MEFs (Fig. 2*B* and *SI Appendix*, Fig. S2*B*). Changes in *Atf4* transcript responded similarly in both genotypes (*SI Appendix*, Fig. S2*B*). Thus, with the exception of the *Atf4* transcript, the relative expression levels of UPR genes increased in response to pharmacological induction of ER stress in the *FicD*^{−/−} MEFs.

Finally, we analyzed how *FicD*[F/F] and *FicD*^{−/−} MEFs responded to and recovered from a physiological stress, glucose starvation. The relative expression levels of *Atf3*, *Chop/Ddit3*, s*XBP1*, *Atf4*, and *FicD* were significantly increased in *FicD*[F/F] MEFs upon starvation and returned to near basal levels after refeeding (Fig. 2*C* and *SI Appendix*, Fig. S2*C*). The relative expression levels of *BiP/HspA5* were also significantly increased in the *FicD*[F/F] MEFs but did not return to basal levels within 4 h of recovery (*SI Appendix*, Fig. S2*C*). The response to this metabolic stress in *FicD*^{−/−} MEFs was dampened, with none of the transcripts elevated to the same extent during glucose starvation. Upon refeeding the *FicD*^{−/−} MEFs, the relative expression levels of *Chop/Ddit3*, s*Xbp1*, and *BiP/HspA5* decreased to basal levels, with patterns similar to those observed in *FicD*[F/F] MEFs (Fig. 2*C* and *SI Appendix*, Fig. S2*C*). Resembling the recovery from DTT-mediated ER stress, *Atf4* levels changed similarly in both genotypes during glucose starvation and refeeding (*SI Appendix*, Fig. S2*C*). However, a distinct expression pattern was observed for *Atf3* transcripts in *FicD*^{−/−} MEFs. After 2 h of refeeding, the *Atf3* transcript level was elevated before lowering back toward basal levels at 4 h of refeeding (Fig. 2*C*). Taken together, relative UPR expression analysis of *FicD*[F/F] and *FicD*^{−/−} MEFs indicates differential regulation under TG, DTT, and glucose starvation conditions, and loss of FicD had significant but distinctive effects under each condition.

Loss of FicD Induces Dramatic Changes in Gene Expression Profiles of MEFs.

We were intrigued by our findings in *FicD*[F/F] MEFs that showed increased BiP AMPylation correlated with strong UPR activation during the physiological stress of glucose starvation (Figs. 1*E* and 2*C*). These observations directly conflict with previous reported AMPylation profiles of BiP and accepted models of FicD catalytic activity for deAMPylation of BiP during
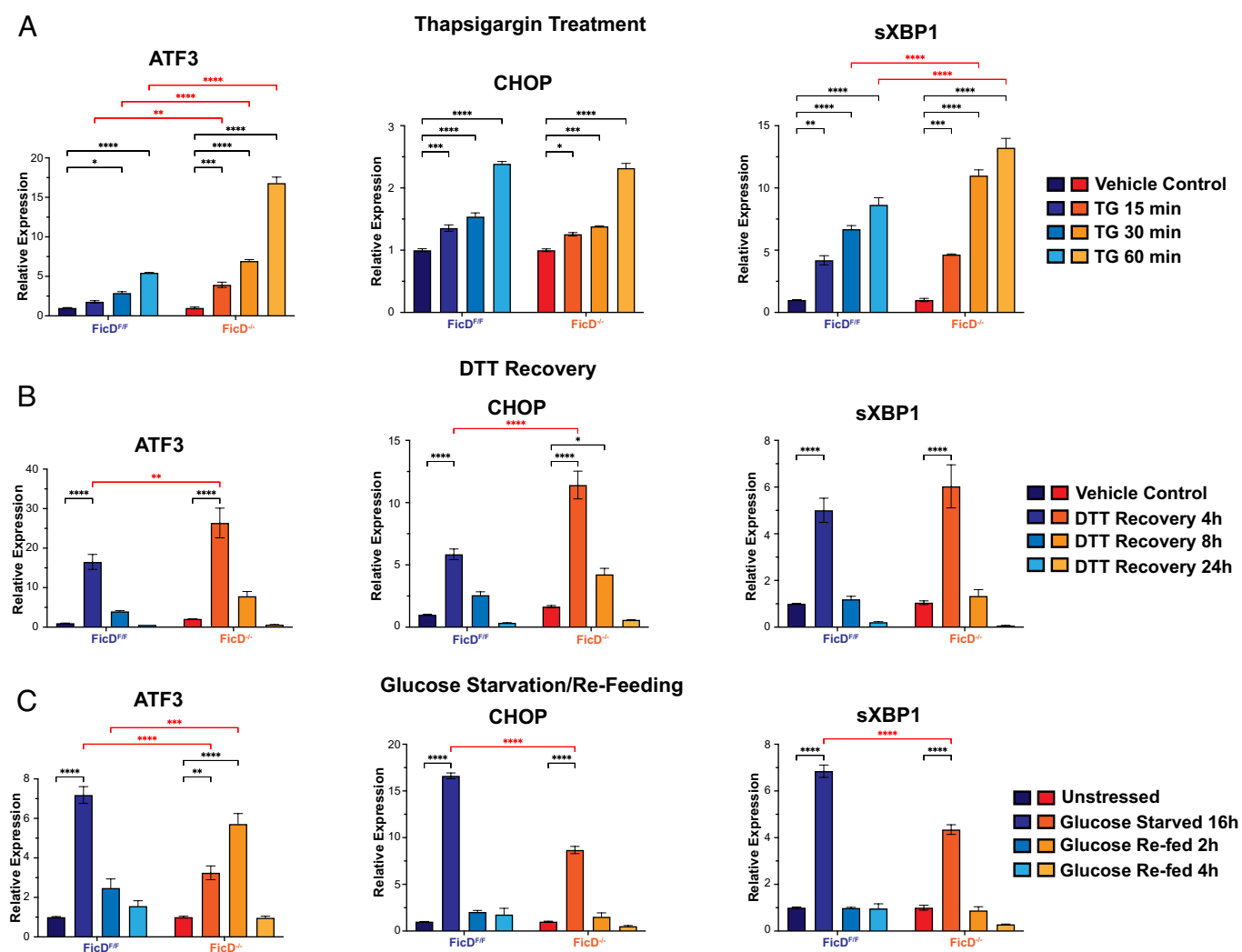
Fig. 2. TG, DTT, and glucose starvation induced ER stress of *FicD*^F/F^ and *FicD*^−/−^ MEFs. RT-qPCR showing relative expression levels of UPR marker genes ATF3, CHOP, and spliced XBP1 (sXBP1) upon (*A*) treatment of MEFs with TG (1 μM), or (*B*) recovery of MEFs from 1 h DTT (5 mM) exposure, or (*C*) glucose starvation (for 16 h) and refeeding of MEFs for indicated time points. Error bars represent the SD of three biologically independent repeat of the experiment with four technical replicates. Genotypes are demonstrated by shades of blue for *FicD*^F/F^ and shades of orange for *FicD*^−/−^ MEFs. Two-way ANOVA with the Tukey multiple comparison test is applied to determine the significance. *P* values: 0.1234 (ns), 0.0332 (*), 0.0021 (**), <0.0001 (****). Nonsignificant comparisons are not shown for clarity.

a pharmacologically induced stress (24, 28–31, 34). In addition, altered UPR gene transcript levels during starvation and recovery in *FicD*^−/−^ MEFs compared to *FicD*^F/F^ MEFs suggested that loss of FicD activity altered the response of these cells to this physiologically relevant stress.

To investigate whether additional molecular pathways could be altered in *FicD*^−/−^ MEFs when compared to *FicD*^F/F^ MEFs under glucose starvation, we performed RNAseq. Data were collected for *FicD*^F/F^ and *FicD*^−/−^ MEFs treated with four different conditions: unstressed (standard growth media), 18 h of glucose starvation; 2 h of glucose refeeding; and 4 h of glucose refeeding (Fig. 3*A*). Principal component analysis (PCA) of all gene counts cluster the biological replicates from each condition, while the clusters for genotypes and treatments segregate. The *FicD*^F/F^ and *FicD*^−/−^ MEF transcriptomes exhibit similar trends relative to metabolic stress treatments. The gene expression response to glucose starvation changes the least compared to unstressed cells. Glucose refeeding at 2-h initiates the largest transcriptome response, and 4 h refeeding trends back toward the unstressed state. Notably, the largest spread of the gene expression data (indicated by PC1) results from a single change, the absence of FicD (Fig. 3*B*). We compared RNA sequencing (RNA-seq) reads from various

pairwise conditions to better understand the transcriptome changes associated with 1) metabolic stress treatment and recovery in *FicD*^F/F^ 2) metabolic stress treatment and recovery in *FicD*^−/−^ MEFs and 3) genotype differences in unstressed and starved MEFs (Fig. 3*C*).

Glucose Starvation Induces PERK-Responsive UPR That Recovers with Refeeding. Differentially expressed genes (DEGs) were defined for *FicD*^F/F^ MEFs subjected to the various treatments (Fig. 3 *A* and *C*, *FicD*^F/F^ metabolic response). The *FicD*^F/F^ glucose-starved cells exhibited 150 significantly up-regulated genes compared to unstressed MEFs, including eight elevated genes classically related to UPR (Fig. 4*A*). The starvation responsive UPR genes from the *FicD*^F/F^ MEFs include those belonging to the PERK modulated cascade leading to apoptosis (*Atf4*, *Atf3*, *Chop/Ddit3*, *Chac1*, *Ero1a*), consistent with our RT-qPCR measurement observed in Fig. 2.

The role of the UPR in the *FicD*^F/F^ MEFs response to glucose starvation is further supported by enriched functions among the up-regulated DEGs (Table 1, UPR terms marked by *). Both starvation responsive terms and UPR associated terms were enriched. In addition, functional overlap between glucose
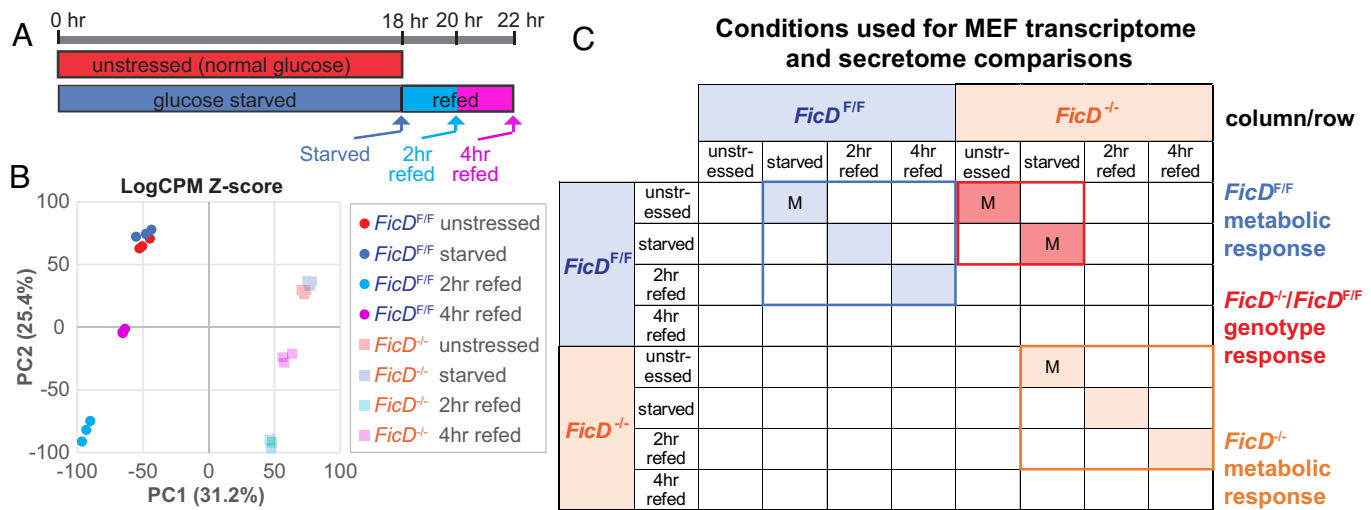
Fig. 3. MEF genotype and metabolic treatment comparisons. (*A*) Timeline of MEF treatments. (*B*) PCA plot of Log2CPM Z-scores for indicated genotypes and treatments in triplicate. (*C*) DEG were calculated by comparison of conditions indicated in rows with respect to conditions in columns. Comparisons indicated by "M" were also compared by MS/MS of secreted proteins.

starvation and UPR DEGs is found in glucose metabolism, in which genes involved in gluconeogenesis (*Gpt2* and *Pck2*) and UPR (*Atf3*, *Atf4*, *Chop/Ddit3*) are enriched.

Next, we compared the DEGs from *FicD*^F/F^ MEFs at 2-h and 4-h glucose refeeding with starved and 2-h refed, respectively. Upon 2-h refeeding, the *FicD*^F/F^ cells showed the largest number of DEGs, highlighting a large transcriptional response upon the reintroduction of glucose. Many of the UPR genes up-regulated during glucose starvation are down-regulated at 2 h of glucose refeeding, suggesting a recovery from the starvation induced UPR (Fig. 4*B*). At 4 h of glucose refeeding, the remainder of the UPR genes (*Atf3* and *Ero1a*), as well as an additional UPR gene (*Thbs1*) that was up-regulated at 2-h refeeding, are lowered toward unstressed levels (Fig. 4*C*).

Upregulation of UPR genes during glucose starvation, followed by downregulation of UPR DEGs during recovery highlights the homeostatic nature of the response to metabolic stress. This observation is further confirmed by the inverse correlation of DEGs from 2-h glucose-refed MEFs (compared to starved cells) to DEGs from 4-h glucose-refed MEFs (compared to 2-h glucose-refed cells) (Fig. 4*D*). One exception in *FicD*^F/F^ MEFs is ATF3; it remains slightly up-regulated at 2 h of glucose refeeding in wild-type cells. Taken together, our RNA-seq analysis is consistent with *FicD*^F/F^ MEFs undergoing metabolic stress and PERK responsive UPR transcription during glucose starvation and undergoing recovery during refeeding.

Transcriptional Response to Glucose Starvation Is Muted in *FicD*^−/−^ MEFs. In contrast to the enhancement of the UPR genes during glucose starvation in *FicD*^F/F^ MEFs (Fig. 4*A*), differential gene expression is almost absent in glucose starved *FicD*^−/−^ MEFs when compared to unstressed *FicD*^−/−^ cells (Fig. 4*E*). DEGs are restricted to 11 genes being up-regulated and 6 genes being down-regulated, with a notable absence of altered UPR gene expression. Although the trend toward lower expression levels for the UPR genes analyzed by RT-qPCR *FicD*^−/−^ MEFs is still observed in the RNA seq data, these genes do not significantly stand out among total transcripts.

To ensure this loss of response was not an artifact of our RNA seq analysis with EdgeR, we compared the EdgeR-defined DEGs to those defined by additional methods (DESeq2, NOISeq, and limma). All four methods exhibited an overlapping gene expression profile for both *FicD*^F/F^ and *FicD*^−/−^ MEFs (*SI Appendix*, Fig. S3 *A* and *B*). The intersection of DEGs defined by all methods represents only three genes, compared to 186 intersecting DEGs in *FicD*^F/F^ MEFs. The top two down-regulated genes in *FicD*^−/−^ MEFs were *Txnip* and *Arrdc4* (Fig. 4*E*), which play roles in suppressing glucose uptake into cells (38). These two genes are down-regulated to a similar extent in the *FicD*^F/F^ MEFs upon glucose starvation. Taken together, the data suggest a loss of differential expression in response to glucose starvation in *FicD*^−/−^ MEFs without directly influencing the maintenance of glucose homeostasis.

Transcriptional Response to Glucose Refeeding Is Robust but Muted in *FicD*^−/−^ MEFs. Though the *FicD*^−/−^ MEFs exhibit a muted transcriptional response during glucose starvation, significant changes in the transcriptional profile are observed in the *FicD*^−/−^ MEFs upon glucose refeeding. Like the transcription response observed for *FicD*^F/F^ MEFs (Fig. 4*B*), the *FicD*^−/−^ MEFs exhibit most DEGs after 2-h glucose refeeding (Fig. 4*F*). In fact, many of the genes that are up-regulated in response to the reintroduction of glucose overlap in the two genotypes (352 overlapping genes represent 58% of up-regulated *FicD*^F/F^ MEFs and 68% of up-regulated *FicD*^−/−^ MEFs genes, *SI Appendix*, Fig. S3*C*). Given this overlap, we observed a similar inverse correlation of 2-h refeeding with 4-h refeeding for *FicD*^−/−^ MEFs genes (Fig. 4*H*). Additionally, down-regulated genes in the *FicD*^−/−^ MEFs upon glucose refeeding (*Crebrf*, *Chac1*, and *Parp16*) overlap with down-regulated UPR genes in the *FicD*^F/F^ MEFs. However, the *Chac1* downregulation in *FicD*^−/−^ MEFs is dampened (40% of starved levels in *FicD*^−/−^ MEFs vs. 4% of starved levels in *FicD*^F/F^ MEFs) due to its selective upregulation in starved *FicD*^F/F^ MEFs. Chac1 encodes the glutathione-specific gamma-glutamylcyclotransferase 1 responsible for glutathione depletion and the proapoptotic effects of the Atf4-Atf3-Ddit3/chop cascade, which is suppressed in starved *FicD*^−/−^ MEFs.

In addition to sequential transcriptome comparisons for glucose refeeding, we compared the glucose refeeding conditions at both timepoints to baseline unstressed conditions (*SI Appendix*, Fig. S3 *D–G*). The UPR genes *Thbs1*, *Ero1a*, *Atf6*, *HspA5* (BiP), *Atf3*, and *Stc2* are all up-regulated while *Chac1* and *Parp16* are down-regulated in *FicD*^F/F^ cells after 2-h glucose refeeding. For *FicD*^−/−^ MEFs at the same timepoint, a slightly different set of UPR genes are up-regulated (*Atf3*, *Stc2*, *Nfe2l2*, and *Creb3l1*) and down-regulated (*Hspa1*, *Chac1*, and *Parp16*). After 4 h of refeeding, no additional UPR
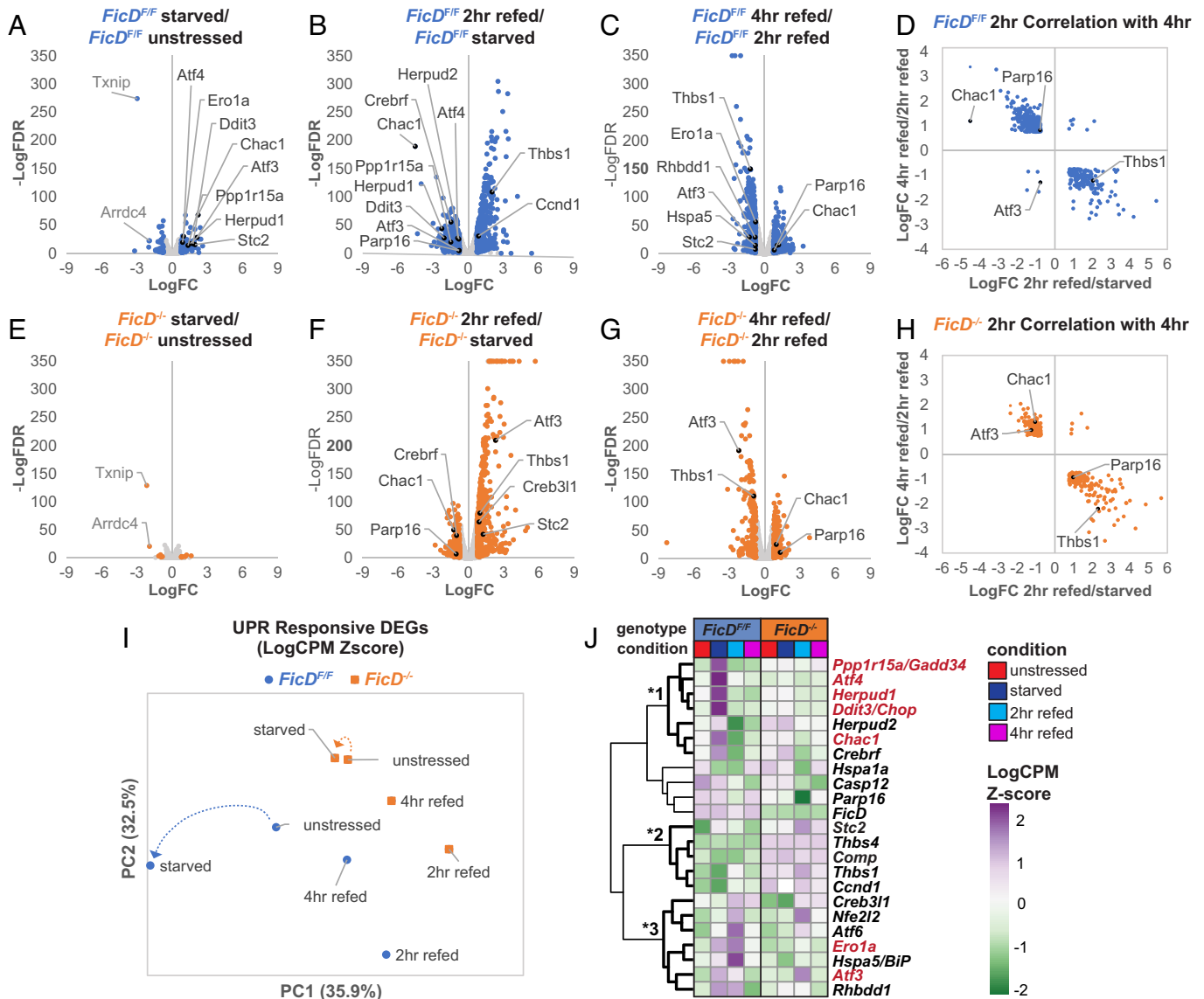
Fig. 4. *FicD*⁻/⁻ MEFs exhibit muted response to homeostatic metabolic stress. (*A–D*) *FicD*^F/F and (*E–H*) *FicD*⁻/⁻ volcano plots (*A–C* and *E–H*) and correlations (*D* and *H*) that highlight RNA-seq comparisons for conditions labeled above graphs, with nodes representing DEGs (blue) or other genes (gray). UPR DEGs (black) and common down-regulated genes in starved cells (gray) are labeled. (*D*) *FicD*^F/F and (*H*) *FicD*⁻/⁻ LogFC inverse correlation between overlapping DEGs for 2-h refed/starved and 4-h refed/2-h refed, with UPR genes labeled. (*I*) PCA plot with arrows pointing toward starved conditions from unstressed conditions and (*K*) heatmap of Log2CPM Z-scores for UPR DEGs, with three clusters indicated by * adjacent to bolded branches. PERK responsive UPR genes are labeled in red.

genes remain significantly up-regulated in the *FicD*^F/F MEFs, while Stc2 and Creb3l1 remain elevated in the FicD⁻/⁻ cells. Given the relatively slower return of these two UPR genes to baseline, we compared the overall DEG count between *FicD*^F/F and *FicD*⁻/⁻ MEFs after glucose refeeding (*SI Appendix*, Fig. S3H). For the *FicD*^F/F MEFs compared to baseline, DEG counts after 2-h refeeding (1,418 genes) lower substantially (487 genes or ~34% of the genes remain altered) after 4-h refeeding. A somewhat less elevated DEG count was observed in the *FicD*⁻/⁻ MEFs after 2-h glucose refeeding (925 genes). This set lowered to 380 DEGs at 4-h refeeding, representing a larger number (~42% of the genes) remaining altered for *FicD*⁻/⁻ MEFs at this timepoint.

Transcriptional UPR Response Mirrors Gluconeogenesis and Is Aberrant in *FicD*⁻/⁻ MEFs. Because UPR genes were noticeably diminished in glucose starved *FicD*⁻/⁻ MEFs, we used PCA and heatmap clustering to examine expression patterns of UPR-specific genes in *FicD*^F/F and *FicD*⁻/⁻ MEFs during glucose starvation

and refeeding. PCA of the UPR-specific genes highlights altered expression levels for *FicD*^F/F MEFs during starvation and refeeding (Fig. 4I). However, for *FicD*⁻/⁻ MEFs, gene expression response to glucose starvation is extremely muted, as illustrated by a comparison of the shifts in each genotype depicted by the dotted arrows (Fig. 4I). A similar clustering of genotype-specific conditions is observed for DEGs involved in gluconeogenesis (*SI Appendix*, Fig. S4A), with the *FicD*^F/F MEFs being more responsive than the *FicD*⁻/⁻ MEFs in the starved condition, and the *FicD*⁻/⁻ MEFs response to glucose refeeding being muted. Approximately one-half of the gluconeogenesis DEGs (nine genes) were significantly up-regulated under glucose starved conditions in *FicD*^F/F MEFs but had little or no response in *FicD*⁻/⁻ MEFs (*SI Appendix*, Fig. S4B). These genes include the UPR transcription factor Atf4, as well as the intracellular leucine sensor (Sesn2) that regulates the mTORC1 signaling pathway (39), the mitochondrial enzyme alanine aminotransferase 2 (Gpt2) that functions in amino acid degradation (40) and the mitochondrial enzyme

Table 1. Enriched GO BP terms for up-regulated DEGs in *FicD*F/F starved/ *FicD*F/F unstressed

GO biological process term name	Adj. *P*-value	Term size	Gene count
Import across plasma membrane	3.222E-05	184	11
Amino acid import across plasma membrane*	3.841E-05	50	7
Response to endoplasmic reticulum stress†	5.709E-05	242	12
Response to hypoxia*	0.0001252	210	11
Amino acid transmembrane transport*	0.0001683	92	8
Endoplasmic reticulum unfolded protein response†	0.0001779	62	7
Intrinsic apoptotic signaling pathway in response to endoplasmic reticulum stress†	0.0001991	63	7
Carboxylic acid transmembrane transport	0.0002304	133	9
Fat cell differentiation*	0.0006416	247	11
Cellular response to hypoxia*	0.0007242	111	8
Negative regulation of multicellular organism growth	0.0022202	14	4
Regulation of transcription from RNA polymerase II promoter in response to stress†	0.0024397	32	5
Positive regulation of transcription from RNA polymerase II promoter in response to stress†	0.0039984	16	4
Basic amino acid transport	0.0052038	17	4
Glucose metabolic process*,†	0.0093236	207	9

*GO terms with starvation-responsive genes.
†GO terms with UPR genes.

phosphoenolpyruvate carboxykinase (Pck2) that serves as the rate-limiting step in glucose production and gluconeogenesis (41).

When examining heat maps of UPR-specific genes, it becomes evident that *FicD*−/− MEFs exhibit either a delayed or dampened UPR response to glucose starvation and refeeding compared to *FicD*F/F MEFs. The UPR genes form three notable clusters (Fig. 4*J*). The first cluster (Fig. 4*J*, *1) includes genes regulated by the PERK arm of the UPR (gene names colored red). This cluster exhibits notable elevation of transcript levels specific to the glucose starved *FicD*F/F MEFs including genes that are slightly elevated in *FicD*−/− starved cells. A second cluster (Fig. 4*J*, *2) includes UPR associated transcripts that are consistently elevated in *FicD*−/− MEFs but not *FicD*F/F MEFs, regardless of the glucose treatment. The third cluster (Fig. 4*J*, *3) of genes is generally elevated in *FicD*F/F MEFs 2-h glucose refed cells, with a subset being elevated also in starved *FicD*F/F MEFs. Only three of the genes in this cluster also exhibit elevated levels in 2-h refed *FicD*−/− MEFs with respect to their unstressed counterparts (Fig. 4*J*). In all three clusters of UPR-specific genes and in both *FicD*F/F and *FicD*−/− MEFs, the 4-h glucose refed state most closely resembled the unstressed conditions, suggesting that MEFs recover from starvation induced UPR by 4 h of glucose refeeding.

FicD Loss Causes Fundamental Changes in the Transcriptome under All Metabolic Conditions. Genotype comparisons across all tested conditions (unstressed, starved, 2 h refed, and 4 h refed) have a significant overlap of DEGs (950 genes) that appears to result from FicD loss (*SI Appendix*, Fig. S4 *C–F*). This overlap can also be seen in the PCA plot (Fig. 3*B*), where the primary principal component PC1 separates the *FicD*F/F from the *FicD*−/− MEFs. Despite this large DEG overlap, the genotype comparisons also include some condition-specific genes. For example, differential expression of the UPR genes *Chac1, Atf3, Atf4, Herpud1, Ddit3* (*Chop*), and *Ppp1r15a* are all specific to the starved *FicD*F/F MEFs (*SI Appendix*, Fig. S4*C*).

We hypothesized that the muted transcriptomic response to glucose starvation in *FicD*−/− MEFs might stem from variations in the baseline unstressed transcriptional profile of these cells. To examine the baseline for *FicD*−/− MEFs, we compared unstressed *FicD*−/− MEFs with unstressed *FicD*F/F MEFs (Fig. 3*C*, *FicD*−/−/*FicD*F/F genotype response). As previously suggested by the transcriptome PCA (Fig. 3*B*), a substantial count of DEGs emerged when comparing the unstressed cells of these two genotypes (Fig. 5*A*), with 852 genes up-regulated and 656 genes down-regulated in *FicD*−/− MEFs. The numerous up-regulated DEGs are enriched in over 180 GO BP terms, only one of which overlaps with the GO BP terms enriched in the *FicD*F/F response to glucose starvation ("fat cell differentiation" in Dataset S1). However, only three fat cell differentiation genes overlap in the two sets: nuclear receptor RorA, transcription factor Klf4, and beta-2-adrenergic receptor Adrb2. This lack of functional enrichment overlap, combined with the transcriptional response profile for UPR (Fig. 4*J*) suggests the muted transcriptomic response to glucose starvation stress in the *FicD*−/− MEFs is unlikely to result from the cells experiencing a baseline glucose-starved state.

To better understand the baseline state of *FicD*−/− cells in relation to the UPR, we compared transcriptional changes in the unstressed state as a representative response to FicD loss (Fig. 5*A*). Among the 852 genes up-regulated in untreated *FicD*−/− MEFs with respect to untreated *FicD*F/F MEFs, 5 are related to UPR. Only one of these UPR genes, *Stc2*, is also up-regulated in the glucose starved *FicD*F/F MEFs (compared to unstressed *FicD*F/F MEFs). *Stc2* encodes a secreted peptide hormone, stanniocalcin-2, whose expression is up-regulated by oxidative stress, hypoxia, and the pharmacological stress inducer TG, supporting the prosurvival function of the UPR (42–44). Only in the *FicD*F/F starved MEFs is the upregulation of *Stc2* accompanied by the PERK arm of the UPR, suggesting that its baseline upregulation in unstressed *FicD*−/− MEFS is a result of an alternate response, potentially related to hypoxic stress (45). Numerous additional hypoxia response genes are differentially regulated between the unstressed *FicD*F/F and *FicD*−/− RNA-seq datasets (102 genes total). A heatmap of their expression levels clusters the genes according to genotype, with roughly one third of the set up-regulated specifically in the *FicD*F/F MEFs, one third up-regulated specifically in the *FicD*−/− MEFS, and one third up-regulated in both genotypes (*SI Appendix*, Fig. S4*G*).
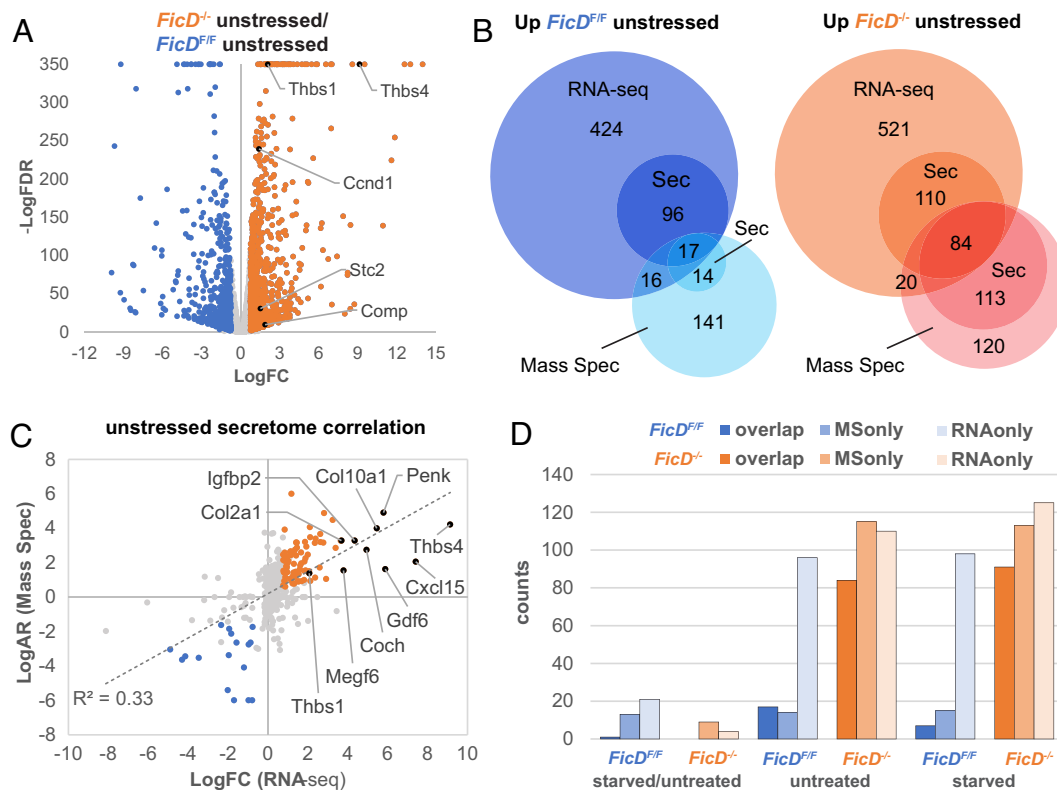
Fig. 5. Genotype comparisons reveal upregulation of secretome in *FicD*⁻/⁻ MEFs. (*A*) Volcano plot highlights RNA-seq genotype comparisons of *FicD*⁻/⁻ unstressed with respect to *FicD*^F/F unstressed MEFs. Nodes represent DEGs up-regulated in *FicD*⁻/⁻ (orange), up-regulated *FicD*^F/F (blue), or other genes (gray). UPR genes are labeled (black). (*B*) Venn diagrams compare all and secreted subset of RNA-sec defined DEGs (RNA) with all and secreted subset of significantly different Mass Spec (MS) identified proteins for unstressed *FicD*^F/F/unstressed *FicD*⁻/⁻ MEFs (blue/cyan shades) and unstressed *FicD*⁻/⁻ MEFs/unstressed *FicD*^F/F MEFs (orange/red shades). (*C*) Correlation of Log2 fold change (LogFC) for secreted transcriptome (RNA-seq) with Log2 abundance ratio for secreted proteome (MS) for all overlapping genes/proteins in *FicD*⁻/⁻ unstressed/*FicD*^F/F unstressed MEFs. Nodes represent *FicD*^F/F up-regulated by both RNA and MS (blue), *FicD*⁻/⁻ up-regulated by both RNA and MS (orange), and others (gray). UPR and other top up-regulated genes in *FicD*⁻/⁻ are labeled. (*D*) Bar graph depicts secreted gene or protein counts defined by both RNA and MS (dark shades), MS only (medium shades), and RNA only (light shades) for the indicated comparisons.

Three of the UPR genes up-regulated by genotype comparison in the unstressed *FicD*⁻/⁻ MEFs (*Thbs4*, *Thbs1*, and *Comp*) encode ECM glycoproteins with thrombospondin type-3 repeats that bind calcium (46). Consistent with the roles of these glycoproteins in the ECM, the top enhanced molecular function terms for the DEGs from the *FicD*⁻/⁻ MEFs that were up-regulated with respect to the *FicD*^F/F MEFs (Table 2) included "ECM structural constituent," "glycosaminoglycan binding," "collagen binding," and other terms describing secreted protein functions. Taken together, our comparison of the unstressed transcriptional profiles of *FicD*^F/F and *FicD*⁻/⁻ MEFs indicate substantial differences in the gene expression patterns of *FicD*⁻/⁻ MEFs and an enrichment in secreted proteins in the absence of FicD.

Increased Protein Secretion in *FicD*⁻/⁻ MEFs. Given the enrichment of transcripts for secreted proteins among up-regulated DEGs in the unstressed *FicD*⁻/⁻ MEFs (compared to unstressed *FicD*^F/F MEFs), we reasoned the absence of FicD and thereby BiP AMPylation may increase the levels of proteins reaching the extracellular space. Previous reports have also suggested that deletion of *FicD* impacts the secretion of cytokines and immunoglobulins in B cells (47). To test this idea, we opted to analyze proteins secreted from both genotypes under unstressed and glucose-starved conditions using tandem mass spectrometry (MS/MS).

First, we defined the overlap between the differentially expressed transcripts identified by RNA-seq and the secreted proteome identified by MS/MS by comparing the genotypes grown under unstressed conditions. Among the DEGs that were elevated in

FicD^F/F compared to *FicD*⁻/⁻ MEFs, approximately one-fifth of the transcripts encoded secreted proteins. Of these, only 17 (3%) were identified as elevated by MS/MS (Fig. 5 *B*, *Left*). A relatively larger proportion of the transcripts elevated in *FicD*⁻/⁻ MEFs compared to *FicD*^F/F MEFs encode secreted proteins (26%), and they exhibit a larger overlap (84 proteins, 12%) with the secreted proteins identified by MS/MS (Fig. 5 *B*, *Right*). Though many of the differentially regulated transcripts observed by RNA seq analysis do not overlap with the altered proteins seen by MS/MS analysis (Fig. 5*B*), a positive correlation ($R^2 = 0.33$ or R = 0.57) exists between transcripts and their overlapping MS/MS identified proteins (Fig. 5*C*). Two of the up-regulated UPR transcripts from *FicD*⁻/⁻ MEFs, Thbs1 and Thbs4, were also detected as secreted proteins by MS/MS.

Next, we compared the secretomes of starved MEFs with to those of the unstressed MEFs. *FicD*^F/F starved cells exhibit slightly elevated levels of secreted proteins and transcripts when compared to unstressed conditions, with little overlap. These levels are both lower in the *FicD*⁻/⁻ MEFs, which have no overlap between identified secreted proteins and their transcripts (Fig. 5*D*, starved/unstressed). These lower levels reflect the muted transcription response of *FicD*⁻/⁻ MEFs in response to starvation (Fig. 4*A*). Despite this muted comparative response, both unstressed and starved *FicD*⁻/⁻ MEFs have elevated secretomes when compared to *FicD*^F/F MEFs under the same conditions (Fig. 5*D*, orange vs. blue).

We conducted a puromycin-based analysis to assess protein synthesis in both *FicD*^F/F and *FicD*⁻/⁻ MEFs, aiming to discern differences in overall translation between the genotypes. Thirty

Table 2. Enriched GO MF terms for up-regulated DEGs in *FicD*⁻/⁻ unstressed/*FicD*F/F unstressed

GO molecular function term name	Adj. *P*-value	Term size	Gene count
ECM structural constituent	9.40E-11	131	26
Glycosaminoglycan binding	1.60E-09	171	28
Heparin binding	2.44E-09	127	24
Integrin binding	9.70E-08	138	23
Collagen binding	5.09E-06	61	14
Sulfur compound binding	2.624E-05	228	26
Adenylyltransferase activity	0.0013221	28	8
Chemorepellent activity	0.0088081	26	7
Cytokine binding	0.0095515	125	15

minutes before harvesting the cells for lysis, we added puromycin to the media to prematurely terminate translation in the cells. Indeed, western blot quantification showed that *FicD*⁻/⁻ MEFs tend to have higher levels of protein synthesis across all tested conditions. Although these differences did not reach statistical significance, the trend suggests an increase in protein synthesis in *FicD*⁻/⁻ MEFs, aligning with our findings (*SI Appendix*, Fig. S6).

Loss of Ire1 Enhances PERK Activity and Alters AMPylation of BiP during Glucose Starvation and Recovery. Finally, we analyzed how *IRE1*⁻/⁻ and *PERK*⁻/⁻ MEFs respond to glucose starvation and recovery (Fig. 6). Western blot analysis revealed that *IRE1*⁻/⁻ MEFs display altered BiP AMPylation patterns during both glucose starvation and recovery. In addition, *IRE1*⁻/⁻ MEFs exhibit signs of enhanced PERK activation during glucose starvation and recovery, both through elevated CHOP production and mobility shifts in PERK protein. In *PERK*⁻/⁻ MEFs, no change in BiP AMPylation patterns were observed during glucose starvation and recovery. However, BiP protein levels were diminished in the *PERK*⁻/⁻ MEFs under all conditions. Taken together, our comparison of wildtype, *IRE1*⁻/⁻, and *PERK*⁻/⁻ MEFs indicates substantial differences in regulation of BiP expression and BiP AMPylation in the absence of these branches of the UPR.

Discussion

BiP is a key player in maintaining protein homeostasis within the ER, and its reversible AMPylation by FicD enzyme has been implicated in modulating its chaperone activity in response to ER stress. The findings presented in this study shed light on the relationship between BiP AMPylation and the UPR response to physiological stress induced by glucose starvation and refeeding. Unlike the ER stress-inducing drugs TG and DTT, glucose starvation led to an induction of PERK responsive UPR transcription that was accompanied by increased BiP AMPylation. Both the UPR response to glucose starvation and BiP AMPylation decreased in *FicD*F/F MEFs upon reintroduction of glucose (Fig. 1 *C–E*). This surprising inverse response of BiP AMPylation to chemical and physiological treatments suggests that different stresses induce distinctive outcomes in modulating the amount of active BiP and the UPR response. Chemical inducers of ER stress are pleotropic, do not necessarily reflect UPR resulting from unfolded proteins, and many times are irreversible and therefore not easily resolved (35, 48). By contrast, deprivation of glucose in MEFs more closely simulates a reversible physiological ER stress. The inverse upregulation of AMPylation under starved conditions emulated the PTM status of BiP in CHX-treated cells with short exposure to DTT stress (Fig. 1*B*). For starvation, it is tempting to speculate that the increase in BiP AMPylation reflects an ER stress-initiated decrease

in protein translation (akin to CHX treatment) to reduce the energetic cost of ER folding and overcome the lower availability of sugar substrates for protein glycosylation.

The lack of BiP AMPylation in *FicD*⁻/⁻ MEFs led to a muted transcription response to glucose starvation and refeeding as measured by qPCR for a few known UPR genes (Fig. 2*C*). To gain a more comprehensive understanding of the impact of FicD on UPR-specific and overall gene expression under metabolic stress, we performed RNA-seq analysis of *FicD*F/F and *FicD*⁻/⁻ MEFs grown in different glucose treatment conditions. The glucose starved *FicD*F/F cells up-regulate transcripts for amino acid import, hypoxia response, and glucose metabolism (Table 1). Initiation of these biological processes suggests the MEFs tolerate glucose starvation by switching their energy source to amino acids, as has been observed in cells exposed to hypoxia (49). The reported hypoxia induced glucose tolerance depended on 5′-AMP-activated protein kinase (AMPK), a well-known stress response activated by glucose starvation. AMPK restores cellular energy balance during stress by sensing intracellular levels of AMP, ADP, and ATP (49, 50). The kinase is activated by mitochondrial stressors that increase the AMP or ADP to ATP ratio in cells. FicD activity could conceivably alter these nucleotide levels during the AMPylation and deAMPylation cycles of BiP, providing a mechanism for ER stressors to influence AMPK and the energetic status of the cell. Glucose starvation of the *FicD*F/F MEFs also increased expression of genes from the PERK arm of the UPR (Fig. 4 *A* and *J*), which is consistent with reported relationships between low glucose levels and induction of the PERK–CHOP pathway (51, 52). The UPR
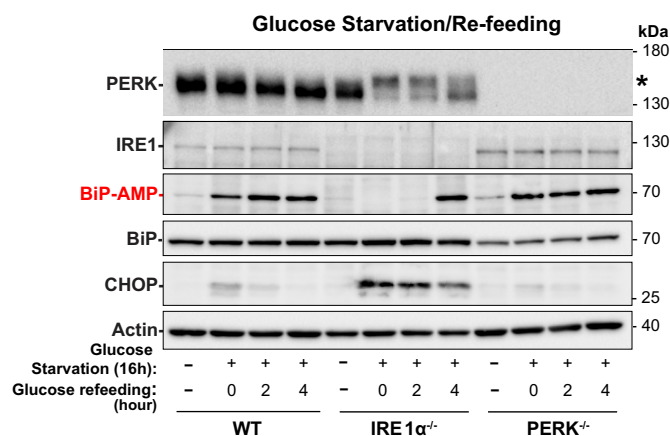

Fig. 6. Loss of IRE1-α alters BiP AMPylation during glucose starvation and recovery. Western blot comparing response of wild-type, *IRE1-α*⁻/⁻, and *PERK*⁻/⁻ MEFs to glucose starvation and refeeding. Asterisk (*) indicates phosphorylated PERK.

induction was muted in the starved *FicD*$^{-/-}$ MEFs, which exhibited limited transcriptional responses to starvation when compared to unstressed cells. This differential transcription response suggests that FicD is essential for mediating a basal response to glucose starvation in MEFs.

The baseline gene expression profile of unstressed *FicD*$^{-/-}$ MEFs differed substantially from that of *FicD*$^{F/F}$ MEFs (Fig. 5*A*), and perhaps this leads to the lack of response to glucose starvation in these cells. Numerous genes encoding secreted ECM and glycosaminoglycan binding proteins were transcriptionally up-regulated in the AMPylation-deficient cells (Table 2). Notably, some of these genes are also associated with the UPR. *Thbs4* transcript was up-regulated 560-fold in *FicD*$^{-/-}$ MEFs from a very low baseline in *FicD*$^{F/F}$ MEFs, while *Thbs1* and *Comp* transcripts were up-regulated 4.2-fold and 3.7-fold, respectively. Thbs4 and Thbs1 function as adhesive glycoproteins in cell-to-cell and cell-to-matrix interactions but also interact with ATF6 in the ER during stress to activate the UPR (53). The Comp protein typically functions in the ECM, but mutations of the *Comp* gene can cause intracellular retention of the protein and activation of the apoptotic arm of the UPR, resulting in skeletal dysplasia (54, 55). Overall, the lack of FicD appears to deregulate the expression of genes and in unstressed cells an elevation of expression is observed for multiple DEGs (Fig. 5 and Table 2).

A single UPR gene, Stanniocalcin-2 (Stc2), was up-regulated in both the glucose-starved *FicD*$^{F/F}$ MEFs and the unstressed *FicD*$^{-/-}$ MEFs. The Stc2 gene encodes a glycosylated peptide hormone that functions as a prosurvival component of the UPR and negatively modulates store-operated Ca^{2+} uptake (43, 44). In response to traditional UPR-inducing drugs tunicamycin and TG, Stc2 expression is up-regulated through the PERK/ATF4 mediated pathway, together with other noted UPR markers (e.g., CHOP/Ddit3_1 and Herpud1) (44). The glucose starved *FicD*$^{F/F}$ MEFs activated similar PERK pathway genes as the tunicamycin/TG treated cells. However, the unstressed *FicD*$^{-/-}$ MEFs activated *Stc2* in the absence of an inducer. This *Stc2* upregulation in the unstressed *FicD*$^{-/-}$ MEFs suggests the inability to AMPylate BiP causes an alternate or premature ER stress. *Stc2* is also up-regulated in response to hypoxia and oxidative stress, and many of the genes that respond to hypoxia are differentially regulated in the RNA-seq dataset (*SI Appendix*, Fig. S2*D*). Among numerous hypoxia response genes whose differential regulation is limited to *FicD*$^{F/F}$ MEFs, *Eif4ebp1* is up-regulated in both starved and 2-h glucose refed states. *Eif4ebp1* is a target of the ATF4 transcription factor and represses translation initiation in response to oxidative stress (56, 57). The dual activation of eIF2α through the UPR and eIF4e through oxidative stress in *FicD*$^{F/F}$ MEFs would reduce translation to levels where BiP is not required for chaperoning and is therefore AMPylated by FicD (58).

Expanding upon our observation of the baseline upregulation of transcripts for extracellular proteins in *FicD*$^{-/-}$ MEFs compared to *FicD*$^{F/F}$ MEFs, we conducted an analysis of protein secretion using tandem mass spectrometry. While the secretome transcript and protein levels correlated, their overlap between the two detection methods remained low in the MEF genotype comparisons (Fig. 5). This low overlap could result from many factors. The abundance of secreted proteins represents a balance of protein synthesis, turnover, and travel through the secretory pathway, that would differ in *FicD*$^{F/F}$ and *FicD*$^{-/-}$ MEFs. The detection of proteins is dependent on the fidelity of detection for a specific peptide and therefore some proteins are overrepresented while others are underrepresented. Despite these limitations, our MS/MS analysis revealed that the abundance of secreted proteins were elevated in *FicD*$^{-/-}$ MEFs when compared to *FicD*$^{F/F}$ MEFs. The comparison

of mRNA levels and MS/MS identification of secreted proteins suggest that *FicD*$^{-/-}$ MEFs secreted a significantly greater quantity of proteins than *FicD*$^{F/F}$ MEFs in both unstressed and starved conditions.

Because inhibition of translation is a primary consequence of UPR signaling, the elevated secretion in *FicD*$^{-/-}$ cells may reflect an inability to constrain protein synthesis. The increased secretome levels in AMPylation-deficient MEFs accompany an increase in protein synthesis observed under all glucose treatment conditions. Thus, protein secretion appears to become dysregulated in *FicD*$^{-/-}$ MEFs where the rheostat for BiP has been deleted. Even under conditions of starvation stress, which usually represses protein translation (59), the hypersecretion response remained unaffected in MEFs lacking FicD. The impaired translation regulation in *FicD*$^{-/-}$ MEFs was also observed in the transcription profile of pre-ribosome genes that function in ribosome biogenesis (*SI Appendix*, Fig. S3*E*). Genes that were up-regulated upon glucose refeeding in *FicD*$^{F/F}$ MEFs, were enriched in the cellular component GO term "preribosome." Most of these genes follow a similar expression pattern trend. They are highest in *FicD*$^{F/F}$ MEFs upon 2 h of feeding and persist at lower levels through 4 h of refeeding. At the same time, their levels are decreased in *FicD*$^{-/-}$ unstressed and starved conditions and elevated slightly after 2 h of refeeding, but not after 4 h. These results provide strong evidence that, in the ER, FicD plays a crucial role in regulating cellular stress responses, transcriptome changes, and the composition of secreted proteins.

Our observations, along with previous studies, propose that the elevated UPR and delayed recovery of the UPR in FicD knockout cells and tissues may be attributed to the excessive chaperoning effect exerted by the heightened active pool of BiP in the absence of FicD. However, the absence of a discernible ERAD gene response in *FicD*$^{-/-}$ MEFs suggests that the elevated UPR and delayed recovery in the absence of FicD may originate primarily from the abundant DEGs in the baseline *FicD*$^{-/-}$ MEFs rather than being solely attributed to excessive chaperone activity of BiP. Moreover, changes in BiP AMPylation patterns in *Ire1*$^{-/-}$ MEFs that coincide with altered PERK activity are suggestive that both of these pathways play a role in the regulation of FicD. This indicates a complex interplay of factors influencing the UPR dynamics in the absence of FicD, where both altered gene expression and the chaperoning effect of BiP may contribute to the observed cellular responses. Overall, these observations support the proposal that a response by the ER is not isolated to the environment of the ER but integrates signals from the cell, similar to previous proposals for an Integrated Stress Response (ISR) (60).

In summary, our study provides compelling evidence for the role of FicD in modulating cellular responses to both pharmacological and physiological ER stress. The absence of FicD leads to alterations in gene expression patterns, disruption of UPR dynamics, abnormal secretion of proteins, and dysregulation of translation; shedding light on the intricate interplay among FicD, ER stress, and cellular homeostasis. These findings emphasize the complexity of the UPR and its sensitivity to diverse stressors. To date, the only validated substrate for FicD mediated AMPylation is BiP. FicD is proposed to act as molecular rheostat for BiP activity. The ability of FicD to control amounts of active BiP by AMPylation and deAMPylation adds additional fidelity to how cells response to UPR. As observed previously, metazoans, such as flies and mice, require this rheostat in tissues composed of differentiated cells essential for an animal's lifetime, such as the eye and pancreas, respectively (30, 31). The presence of this rheostat is necessary to safeguard these tissues from lifelong stress cycles. Further research is needed to elucidate the precise mechanisms through which

FicD's impact extends beyond ER stress and to investigate the functional significance of the observed gene expression changes in the context of ER stress and the more far-reaching ISR (60). Our study provides valuable insights into the molecular pathways governing cellular responses to physiological stress and highlights potential genes and pathways for therapeutic interventions in diseases associated with dysregulated ER stress.

Materials and Methods

Detailed descriptions of the experimental methods are provided in *SI Appendix, SI Materials and Methods*. These include Reagents and general remarks, Isolation and immortalization of MEFs, Cell culture, Cell Harvesting and Lysis, Protein Synthesis Assay, Western-blotting, RNA isolation, RT-qPCR, RNA-seq, Analysis of RNA-seq, Preparation of Secretomes, Tandem Mass Spectrometry, and Analysis of Secretomes.

Data, Materials, and Software Availability. All study data are included in the article and/or supporting information.

Author affiliations: [a]Department of Molecular Biology, University of Texas Southwestern Medical Center, Dallas, TX 75390; [b]HHMI, Dallas, TX 75390; and [c]Department of Biochemistry, University of Texas Southwestern Medical Center, Dallas, TX 75390

1. P. Walter, D. Ron, The unfolded protein response: From stress pathway to homeostatic regulation. *Science* **334**, 1081–1086 (2011).
2. C. Hetz, K. Zhang, R. J. Kaufman, Mechanisms, regulation and functions of the unfolded protein response. *Nat. Rev. Mol. Cell Biol.* **21**, 421–438 (2020).
3. B. M. Gardner, D. Pincus, K. Gotthardt, C. M. Gallagher, P. Walter, Endoplasmic reticulum stress sensing in the unfolded protein response. *Cold Spring Harb. Perspect. Biol.* **5**, a013169 (2013).
4. A. Bertolotti, Y. Zhang, L. M. Hendershot, H. P. Harding, D. Ron, Dynamic interaction of BiP and ER stress transducers in the unfolded-protein response. *Nat. Cell Biol.* **2**, 326–332 (2000).
5. S. Luo, C. Mao, B. Lee, A. S. Lee, GRP78/BiP is required for cell proliferation and protecting the inner cell mass from apoptosis during early mouse embryonic development. *Mol. Cell Biol.* **26**, 5688–5697 (2006).
6. M. Schroder, R. J. Kaufman, The mammalian unfolded protein response. *Annu. Rev. Biochem.* **74**, 739–789 (2005).
7. S. C. Chang, A. E. Erwin, A. S. Lee, Glucose-regulated protein (GRP94 and GRP78) genes share common regulatory domains and are coordinately regulated by common trans-acting factors. *Mol. Cell Biol.* **9**, 2153–2162 (1989).
8. Y. Kozutsumi, M. Segal, K. Normington, M. J. Gething, J. Sambrook, The presence of malfolded proteins in the endoplasmic reticulum signals the induction of glucose-regulated proteins. *Nature* **332**, 462–464 (1988).
9. J. Lee, U. Ozcan, Unfolded protein response signaling and metabolic diseases. *J. Biol. Chem.* **289**, 1203–1211 (2014).
10. S. W. Park, U. Ozcan, Potential for therapeutic manipulation of the UPR in disease. *Semin. Immunopathol.* **35**, 351–373 (2013).
11. M. K. Brown, N. Naidoo, The endoplasmic reticulum stress response in aging and age-related diseases. *Front. Physiol.* **3**, 263 (2012).
12. A. K. Casey *et al.*, Fic-mediated deAMPylation is not dependent on homodimerization and rescues toxic AMPylation in flies. *J. Biol. Chem.* **292**, 21193–21204 (2017).
13. L. A. Perera *et al.*, An oligomeric state-dependent switch in the ER enzyme FICD regulates AMPylation and deAMPylation of BiP. *EMBO J.* **38**, e102177 (2019).
14. B. Gulen, A. Itzen, Revisiting AMPylation through the lens of Fic enzymes. *Trends Microbiol.* **30**, 350–363 (2022).
15. A. K. Casey, K. Orth, Enzymes involved in AMPylation and deAMPylation. *Chem. Rev.* **118**, 1199–1215 (2018).
16. C. Hedberg, A. Itzen, Molecular perspectives on protein adenylylation. *ACS Chem. Biol.* **10**, 12–21 (2015).
17. B. Gulen *et al.*, Identification of targets of AMPylating Fic enzymes by co-substrate-mediated covalent capture. *Nat. Chem.* **12**, 732–739 (2020).
18. C. A. Worby *et al.*, The fic domain: Regulation of cell signaling by adenylylation. *Mol. Cell* **34**, 93–103 (2009).
19. M. P. Müller *et al.*, The Legionella effector protein DrrA AMPylates the membrane traffic regulator Rab1b. *Science* **329**, 946–949 (2010).
20. H. S. Kingdon, B. M. Shapiro, E. R. Stadtman, Regulation of glutamine synthetase, VIII. ATP: Glutamine synthetase adenylyltransferase, an enzyme that catalyzes alterations in the regulatory properties of glutamine synthetase. *Proc. Natl. Acad. Sci. U.S.A.* **58**, 1703–1710 (1967).
21. M. L. Yarbrough *et al.*, AMPylation of Rho GTPases by Vibrio VopS disrupts effector binding and downstream signaling. *Science* **323**, 269–272 (2009).
22. U. Rosani, S. De Felice, R. Frizzo, S. Kawato, K. M. Wegner, FicD genes in invertebrates: A tale of transposons, pathogenic and integrated viruses. *Gene* **893**, 147895 (2023).
23. R. Sengupta, M. J. Poderycki, S. Mattoo, CryoAPEX–An electron tomography tool for subcellular localization of membrane proteins. *J. Cell Sci.* **132**, jcs222315 (2019).
24. H. Ham *et al.*, Unfolded protein response-regulated Drosophila Fic (dFic) protein reversibly AMPylates BiP chaperone during endoplasmic reticulum homeostasis. *J. Biol. Chem.* **289**, 36059–36069 (2014).
25. A. Sanyal *et al.*, A novel link between Fic (filamentation induced by cAMP)-mediated adenylylation/AMPylation and the unfolded protein response. *J. Biol. Chem.* **290**, 8482–8499 (2015).
26. J. Fauser *et al.*, Specificity of AMPylation of the human chaperone BiP is mediated by TPR motifs of FICD. *Nat. Commun.* **12**, 2426 (2021).
27. L. A. Perera *et al.*, Structures of a deAMPylation complex rationalise the switch between antagonistic catalytic activities of FICD. *Nat. Commun.* **12**, 5004 (2021).
28. S. Preissler *et al.*, AMPylation matches BiP activity to client protein load in the endoplasmic reticulum. *Elife* **4**, e12621 (2015).
29. S. Preissler, C. Rato, L. Perera, V. Saudek, D. Ron, FICD acts bifunctionally to AMPylate and de-AMPylate the endoplasmic reticulum chaperone BiP. *Nat. Struct. Mol. Biol.* **24**, 23–29 (2017).
30. A. T. Moehlman, A. K. Casey, K. Servage, K. Orth, H. Kramer, Adaptation to constant light requires Fic-mediated AMPylation of BiP to protect against reversible photoreceptor degeneration. *Elife* **7**, e38752 (2018).
31. A. K. Casey *et al.*, Fic-mediated AMPylation tempers the unfolded protein response during physiological stress. *Proc. Natl. Acad. Sci. U.S.A.* **119**, e2208317119 (2022).
32. M. C. Truttmann *et al.*, The Caenorhabditis elegans protein FIC-1 is an AMPylase that covalently modifies heat-shock 70 family proteins, translation elongation factors and histones. *PLoS Genet.* **12**, e1006023 (2016).
33. L. A. Perera, D. Ron, AMPylation and endoplasmic reticulum protein folding homeostasis. *Cold Spring Harb. Perspect. Biol.* **15**, a041265 (2023).
34. J. E. Chambers, K. Petrova, G. Tomba, M. Vendruscolo, D. Ron, ADP ribosylation adapts an ER chaperone response to short-term fluctuations in unfolded protein load. *J. Cell Biol.* **198**, 371–385 (2012).
35. J. Lytton, M. Westlin, M. R. Hanley, Thapsigargin inhibits the sarcoplasmic or endoplasmic reticulum Ca-ATPase family of calcium pumps. *J. Biol. Chem.* **266**, 17067–17071 (1991).
36. J. R. Subjeck, T. T. Shyy, Stress protein systems of mammalian cells. *Am. J. Physiol. Cell Physiol.* **250**, C1–C17 (1986).
37. D. Scheuner, R. J. Kaufman, The unfolded protein response: A pathway that links insulin demand with beta-cell failure and diabetes. *Endocr. Rev.* **29**, 317–333 (2008).
38. B. R. Wilde, Z. Ye, T. Y. Lim, D. E. Ayer, Cellular acidosis triggers human MondoA transcriptional activity by driving mitochondrial ATP production. *Elife* **8**, e40199 (2019).
39. A. V. Budanov, M. Karin, p53 target genes sestrin1 and sestrin2 connect genotoxic stress and mTOR signaling. *Cell* **134**, 451–460 (2008).
40. M. R. Martino *et al.*, Silencing alanine transaminase 2 in diabetic liver attenuates hyperglycemia by reducing gluconeogenesis from amino acids. *Cell Rep.* **39**, 110733 (2022).
41. A. Abulizi *et al.*, Multi-tissue acceleration of the mitochondrial phosphoenolpyruvate cycle improves whole-body metabolic health. *Cell Metab.* **32**, 751–766.e11 (2020).
42. R. Huber, O. Epp, H. Formanek, Structures of deoxy- and carbonmonoxy-erythrocruorin. *J. Mol. Biol.* **52**, 349–354 (1970).
43. W. Zeiger *et al.*, Stanniocalcin 2 is a negative modulator of store-operated calcium entry. *Mol. Cell Biol.* **31**, 3710–3722 (2011).
44. D. Ito *et al.*, Characterization of stanniocalcin 2, a novel target of the mammalian unfolded protein response with cytoprotective properties. *Mol. Cell Biol.* **24**, 9456–9469 (2004).
45. N. T. Chee, I. Lohse, S. P. Brothers, mRNA-to-protein translation in hypoxia. *Mol. Cancer* **18**, 49 (2019).
46. J. C. Adams, J. Lawler, The thrombospondins. *Int. J. Biochem. Cell Biol.* **36**, 961–968 (2004).
47. N. McCaul *et al.*, Deletion of mFICD AMPylase alters cytokine secretion and affects visual short-term learning in vivo. *J. Biol. Chem.* **297**, 100991 (2021).
48. T. J. Bergmann *et al.*, Chemical stresses fail to mimic the unfolded protein response resulting from luminal load with unfolded polypeptides. *J. Biol. Chem.* **293**, 5600–5612 (2018).
49. H. Esumi *et al.*, Hypoxia and nitric oxide treatment confer tolerance to glucose starvation in a 5′-AMP-activated protein kinase-dependent manner. *J. Biol. Chem.* **277**, 32791–32798 (2002).
50. E. Trefts, R. J. Shaw, AMPK: Restoring metabolic homeostasis over space and time. *Mol. Cell* **81**, 3677–3690 (2021).
51. Y. Gao *et al.*, PERK is required in the adult pancreas and is essential for maintenance of glucose homeostasis. *Mol. Cell Biol.* **32**, 5129–5139 (2012).
52. S. G. de la Cadena, K. Hernandez-Fonseca, I. Camacho-Arroyo, L. Massieu, Glucose deprivation induces reticulum stress by the PERK pathway and caspase-7- and calpain-mediated caspase-12 activation. *Apoptosis* **19**, 414–427 (2014).
53. J. M. Lynch *et al.*, A thrombospondin-dependent pathway for a protective ER stress response. *Cell* **149**, 1257–1268 (2012).

54. K. A. Pirog-Garcia et al., Reduced cell proliferation and increased apoptosis are significant pathological mechanisms in a murine model of mild pseudoachondroplasia resulting from a mutation in the C-terminal domain of COMP. *Hum. Mol. Genet.* **16**, 2072–2088 (2007).

55. Y. Hashimoto, T. Tomiyama, Y. Yamano, H. Mori, Mutation (D472Y) in the type 3 repeat domain of cartilage oligomeric matrix protein affects its early vesicle trafficking in endoplasmic reticulum and induces apoptosis. *Am. J. Pathol.* **163**, 101–110 (2003).

56. S. Yamaguchi et al., ATF4-mediated induction of 4E-BP1 contributes to pancreatic beta cell survival under endoplasmic reticulum stress. *Cell Metab.* **7**, 269–276 (2008).

57. R. Tominaga et al., The JNK pathway modulates expression and phosphorylation of 4E-BP1 in MIN6 pancreatic beta-cells under oxidative stress conditions. *Cell Biochem. Funct.* **28**, 387–393 (2010).

58. H. D. Ryoo, D. Vasudevan, Two distinct nodes of translational inhibition in the Integrated Stress Response. *BMB Rep.* **50**, 539–545 (2017).

59. C. G. Proud, Regulation of mammalian translation factors by nutrients. *Eur. J. Biochem.* **269**, 5338–5349 (2002).

60. M. Costa-Mattioli, P. Walter, The integrated stress response: From mechanism to disease. *Science* **368**, eaat5314 (2020).